



Multi-dimensional fluctuation analysis of target residue in nuclear collisions

Dipak Ghosh*, Argha Deb, Keya Chattopadhyay(Dutta), Srimonti Dutta and Madhumita Banerjee Lahiri

Nuclear and Particle Physics Research Centre, Department of Physics, Jadavpur University, Kolkata-700 032, India

E-mail: dipakghosh_in@yahoo.com

Received 19 December 2005, accepted 19 May 2006

Abstract : This paper presents a detail investigation of fluctuation pattern of the target fragments emitted in the interactions in a wide range of projectile energies from 4.5 AGeV to 200 AGeV. More precisely, fluctuation of target residue is studied in the view of two-dimensional factorial moment methodology using the concept of Hurst exponent (H) to take care of anisotropy of phase space. This study shows that for low projectile energy, the fluctuation pattern is self-similar in most of the bins (*scale*) while self-affine in only one bin region (*scale*); while for the high projectile energy, the fluctuation pattern is self-affine in all the considered bin regions. Thus with increase in the projectile energy, the fluctuation pattern tends to become self-affine. The dependence is observed not only in the degree of anisotropy but also on the strength of fluctuation. The values of α_q are widely different in the different bins at 200 AGeV. However at 4.5 AGeV, the change of α_q from one bin to the other is not as significant as in the former case. Thus, the fluctuation of target residue is scale-dependent and the scale-dependence is more pronounced at the ultra-relativistic energy.

Keywords : Nuclear collisions, target fragments, fluctuation, self-affinity, self-similarity

PACS Nos : 25.75.-q, 24.60.Ky, 25.70.Mn

1 Introduction

Bialas and Peschanskiy [1] made a breakthrough in the field of High energy Physics in 1986 by introducing the concept of intermittency to study large non-statistical fluctuations of pions produced in high energy cosmic ray interactions. They introduced a method for the analysis of large fluctuation which is based on the computation of scaled factorial moment (SFM) in the limit of small phase space intervals. This method proved to be magical in filtering out the statistical noise which was the main problem with the ordinary moment method. Application of this method to JACEE events not only confirmed the prediction of statistical fluctuation but also supplied evidence for a power law dependence of fluctuation on phase space bin size, which was termed intermittency in analogy with the phenomenon in the hydrodynamics of turbulent fluid flow [2]. It is believed that in the pionisation process at ultra-relativistic nucleus-nucleus collisions, the presence of intermittent type of fluctuation is due to QGP phase transition. But evidences of intermittent type of

fluctuations are obtained in low energy nucleus-nucleus collisions also [3], where the existence of QGP phase transition is not expected. Even in the target fragmentation process, the presence of intermittent type of fluctuation has been reported [4,5]. So the QGP phase transition cannot be the only reason for the intermittent type of fluctuation. The presence of random cascade mechanism or conventional short-range correlation may also be responsible for intermittency. Several authors have sought to interpret the intermittent type of fluctuations from known or conjectured properties of particle correlations [6-9]. Most of the data analyses have been carried out for the produced pions but the analysis of the data of target fragments will also provide useful information about the production process.

Analysis of target associated particles, grey and black tracks in emulsion in heavy-ion interaction is scanty. The black tracks are of interest to us in the present analysis. They are identified as target evaporation particles in a model referred to as the 'evaporation model' [10]. In the

*responding Author

evaporation model, the particles corresponding to 'shower' and 'grey' tracks are emitted from the nucleus very soon after the instant of impact, leaving the hot residual nucleus in an excited state. Emission of particles from this state takes place relatively slowly. In order to escape from this residual nucleus, a particle must await a favourable statistical fluctuation, as a result of random collisions between the nucleons within the nucleus, which takes the particle close to the nuclear boundary, traveling in an outward direction and with a kinetic energy greater than the binding energy of the nucleus. After evaporation of this particle, a second particle is brought to a favourable condition for evaporation and so on, until the excitation energy of the residual nucleus is so small that the transition to the ground state is likely to be affected by the emission of γ rays. In the rest system of the nucleus in this model, the directions of emission of the evaporation particles are distributed isotropically. In different experiments, however, the isotropicity has been found to be disturbed, which may be due to loss of kinetic energy of the residual nucleus through ionization, following the impulse of the collision, before the evaporation process is completed [10].

The evaporation model is based on the assumption that the statistical equilibrium has been established in the decaying system and that the lifetime of the system is much longer than the time taken to distribute the energy among the nucleons in the nucleus. However, the concept of the evaporation model has not been universally accepted. Barkas [11] suggested that the mechanisms other than evaporation process must also be considered to explain the emission of all heavy fragments. Different experimental data also indicate the existence of the non-equilibrium nature of the processes to be responsible for the emission of slow, target associated particles.

In earlier times, most of the studies on fluctuation pattern of pions and target fragments were performed in one-dimensional space, whereas real process occurs in three dimensions. So this one-dimensional analysis is unable to extract any conclusion on the complete dynamical fluctuation pattern. Ochs [12] remarked that in a lower dimensional projection, the fluctuation is reduced by the averaging process. The projection effect may completely wash out the self-similar nature of fluctuations. In two-dimensional analysis, generally the phase spaces are equally divided in both directions assuming the isotropic nature of phase space. However, Van Hove [13] indicated that the phase space in multiparticle production process is anisotropic. The longitudinal momenta are usually large

while the transverse ones are limited to small values. This view is extended to the fragmentation process. It is expected that the fluctuations should also be anisotropic and the scaling behaviour is different in different directions giving rise to self-affine scaling. It is therefore essential to see the fluctuation pattern of target fragments considering anisotropy of phase space.

Earlier, we have studied [14] the fluctuation pattern of target fragments of ^{24}Mg -AgBr interaction at 4.5 AGeV in complete $(\eta - \phi)$ phase space and the study revealed that fluctuation pattern is self-affine with Hurst exponent $H = 0.7$. For ^{32}S -AgBr interaction, the study revealed that the fluctuation pattern is self-affine with $H = 0.3$ in complete $(\eta - \phi)$ phase space [15]. In this work, we have studied the 'scale dependence' of fluctuation pattern of target fragments emitted in ^{24}Mg -AgBr interactions at 4.5 AGeV and ^{32}S -AgBr interactions at 200 AGeV. We have also tried to observe that whether this scale dependence of fluctuation pattern is a general behaviour and whether or not it depends on the projectile energy.

2. Experimental details

We have performed our analysis on the interactions initiated by ^{24}Mg -AgBr at 4.5 AGeV and ^{32}S -AgBr interactions at 200 AGeV. The data set used in this analysis was obtained by exposing NIKFI BR2 nuclear emulsion plates to ^{24}Mg beam at 4.5 AGeV at JINR, Dubna and G5 nuclear emulsion plates to ^{32}S beam at 200 AGeV from CERN, SPS.

The particles emitted after interaction are classified as

- (i) Black particles which are constituted of target fragments. They have range < 3 mm and velocity < 0.3 c.
- (ii) Grey particles which are constituted of recoil proton with energy upto 400 MeV. They have range > 3 mm and velocity between 0.3 c and 0.7 c.
- (iii) Shower particles which are mainly constituted of produced pions. They have velocity > 0.7 c.

Along with these tracks, there are few projectile fragments. They generally lie within 3° with respect to main beam direction. Great care is taken to identify the projectile fragments.

A total of 800 events for ^{24}Mg beam (with an average multiplicity 10.09) and 140 events for ^{32}S beam (with an average multiplicity 9.68) with $n_h \geq 8$ were selected for the present analysis as genuine ^{24}Mg -AgBr and ^{32}S -AgBr interactions ($n_h = n_b + n_g$). The details of the data scanning and measurement procedure is given in earlier papers [15,16]. It is worthwhile to mention that

emulsion technique possesses very high spatial resolution which makes it a very effective detector though with limited statistics

3. Method of study

For two dimensional analysis of fluctuation pattern of target fragments, we first consider the two dimensional factorial moment defined by the relation (1). In two-dimensional phase space, if the two phase space variables are x_1 and x_2 , factorial moment of order q , F_q is given by the relation

$$F_q(\delta x_1, \delta x_2) = \frac{1}{M'} \sum_{m=1}^M \frac{n_m(n_m-1) \dots (n_m-q+1)}{\langle n_m \rangle^q} \quad (1)$$

where $(\delta x_1, \delta x_2)$ is the size of a two dimensional cell, n_m the multiplicity in the m -th cell M' is the number of two-dimensional cells into which the considered phase-space has been divided

$$\delta x_1 = \Delta x_1 / M_1, \quad (2)$$

$$\delta x_2 = \Delta x_2 / M_2, \quad (3)$$

M_1 and M_2 are the scale factors in direction x_1 and x_2 . $M_1 \neq M_2$ and $M' = M_1 M_2$

M_1 and M_2 satisfy the equation

$$M_1 = M_2^H, \quad (4)$$

where the parameter H ($0 < H \leq 1$) is called Hurst exponent [17]. It is the parameter which characterizes the self-affine property of dynamical fluctuations. It is clear from eq (4) that the scale factors M_1 and M_2 cannot simultaneously be integer, so that the size of elementary phase space cell should be able to take continuously varying values

For performing the analysis with non-integral value of scale factor (M), we adopt the following method. For simplicity consider one-dimensional space (y) and let

$$M = N + a, \quad (5)$$

where N is an integer and $0 \leq a < 1$. When we use the elementary bin of width $\delta y = \Delta y / M$ as 'scale' to 'measure' the region Δy , we get N of them and a smaller bin of width $a\Delta y / M$ left. Putting the smaller bin at the last (or first) place of the region and doing the average with only the first (or last) N bins, we have

$$F_q(\delta x) = \frac{1}{N} \sum_{n=1}^N \frac{n(n-1) \dots (n-q+1)}{\langle n \rangle^q} \quad (6)$$

M determined by eq (5), can be any positive real number and so can vary continuously

Our work has been performed in two-dimensional $\cos(\theta) - \phi$ space (w.r.t. the beam direction), where the values of $\cos(\theta)$ is from -1 to $+1$ and the azimuthal region is 0 to 2π . As shape of this distribution influences the scaling behavior of the factorial moments, we have used the 'cumulative' variable [18] $X_{\cos\theta}$ and X_ϕ instead of $\cos\theta$ and ϕ . The corresponding region of investigation for both the variables then become $(0,1)$. The cumulative variable $X(x)$ is given by the relation as below

$$X(x) = \int_0^x \rho(x') dx' / \int_0^1 \rho(x') dx', \quad (7)$$

where x_1 and x_2 are two extreme points in the distribution $\rho(x)$, between which X varies from 0 to 1 . However to avoid confusion, we have called the variables $X_{\cos\theta}$ and X_ϕ as $\cos(\theta)$ and ϕ and later in this paper, wherever we mention $\cos(\theta)$ and ϕ , we actually mean $X_{\cos\theta}$ and X_ϕ .

We have calculated the factorial moments for the q -th order with the varying values of Hurst components. The scale factors in longitudinal and transverse directions are chosen as

$M_F = 2, 3, \dots, 30$ for $^{24}\text{Mg-AgBr}$ interactions,

$M_F = 6, 7, \dots, 26$ for $^{32}\text{S-AgBr}$ interactions and $M_n = M_F^H$

We have not considered the first data point corresponding to $M_F = 1$ to reduce the effect of momentum conservation [18] which tends to spread the particle in opposite directions and thus reduce the value of factorial moments. This effect becomes weaker with higher values.

The intermittent behavior of multiplicity distribution manifests itself as the power law-dependence of factorial moment on the cell size as the cell size $\rightarrow 0$

$$\langle F_q \rangle \propto (\delta(\cos(\theta)\delta\phi))^{-\alpha}.$$

The exponent α_q is the slope characterizing linear rise of $\ln\langle F_q \rangle$ with $-\ln(\delta(\cos(\theta)\delta\phi))$.

The strength of the intermittency is characterized by the exponent α_q can be obtained from the linear fit of the form

$$\ln\langle F_q \rangle = -\alpha_q \ln(\delta(\cos(\theta)\delta\phi)) + A \quad (8)$$

where A is a constant.

We have plotted $\ln\langle F_q \rangle$ vs. $-\ln(\delta(\cos(\theta)\delta\phi))$ for different values of H . We have calculated the values of $\chi^2/d.o.f$. We have optimized the value of H by finding out the minimum of $\chi^2/d.o.f$.

4. Results and discussion

We have plotted the natural logarithm of $(\delta \cos \theta) \delta \phi$ along X -axis and natural logarithm of average value of factorial moments of order q ($q = 2-5$) along Y -axis for different Hurst components starting from $H = 0.3$ to $H = 0.7$ by steps of 0.1 and for $H = 1$ in bin region 2–30 for ^{24}Mg -AgBr interactions. In order to find the partition condition at which the anisotropic behavior is best revealed, we have performed the linear best fit and χ^2 per degree of freedom is calculated.

H where self-affinity or self-similarity occurs, are given in Table 3.

Figures 1(a) and (b) show the variation of natural logarithm of $(\delta \cos \theta) \delta \phi$ and natural logarithm of average value of factorial moments of order q ($q = 2, \dots, 5$) for bin range $2 \leq M \leq 30$ for $H = 1.0$ and $H = 0.3$ respectively. The error bars denote the statistical errors. Figure 2(a,b,c) show the same for bin ranges $2 \leq M \leq 15$, $10 \leq M \leq 20$ and $12 \leq M \leq 25$ respectively for $H = 1.0$. Similar variation has been shown for bin region $15 \leq M \leq 30$ in

Table 1. The values of χ^2/dof in different bins for $q = 2-5$ for different Hurst exponent H for ^{24}Mg -AgBr interactions

| H | q | Values of χ^2/dof | | | | |
|-----|-----|-------------------------------|--------------------|---------------------|---------------------|---------------------|
| | | $2 \leq M \leq 30$ | $2 \leq M \leq 15$ | $15 \leq M \leq 30$ | $10 \leq M \leq 20$ | $12 \leq M \leq 25$ |
| 0.3 | 2 | 1.705 | 1.475 | 0.078 | 0.524 | 0.057 |
| | 3 | 1.800 | 1.806 | 0.080 | 0.581 | 0.085 |
| | 4 | 1.110 | 1.437 | 0.104 | 0.538 | 0.096 |
| | 5 | 0.726 | 1.221 | 0.145 | 0.504 | 0.146 |
| 0.4 | 2 | 0.882 | 1.075 | 0.083 | 0.147 | 0.135 |
| | 3 | 1.494 | 1.373 | 0.180 | 0.340 | 0.313 |
| | 4 | 1.514 | 1.028 | 0.267 | 0.533 | 0.484 |
| | 5 | 4.093 | 0.802 | 0.304 | 0.608 | 0.555 |
| 0.5 | 2 | 0.453 | 0.521 | 0.263 | 0.287 | 0.255 |
| | 3 | 1.860 | 1.090 | 0.538 | 0.455 | 0.456 |
| | 4 | 2.508 | 1.478 | 0.803 | 0.683 | 0.702 |
| | 5 | 3.117 | 1.721 | 1.042 | 0.798 | 0.891 |
| 0.6 | 2 | 0.697 | 0.758 | 0.200 | 0.252 | 0.201 |
| | 3 | 1.737 | 1.872 | 0.410 | 0.512 | 0.441 |
| | 4 | 2.546 | 3.016 | 0.574 | 0.877 | 0.647 |
| | 5 | 3.707 | 4.207 | 0.701 | 1.178 | 0.826 |
| 0.7 | 2 | 0.584 | 0.258 | 0.344 | 0.227 | 0.269 |
| | 3 | 1.508 | 1.219 | 0.436 | 0.369 | 0.317 |
| | 4 | 2.648 | 3.007 | 0.509 | 0.397 | 0.379 |
| | 5 | 4.097 | 5.076 | 0.500 | 0.416 | 0.334 |
| 1.0 | 2 | 0.448 | 0.155 | 0.256 | 0.133 | 0.090 |
| | 3 | 1.286 | 0.740 | 0.095 | 0.153 | 0.130 |
| | 4 | 2.044 | 1.922 | 0.097 | 0.221 | 0.159 |
| | 5 | 2.939 | 3.897 | 0.081 | 0.206 | 0.148 |

For ^{24}Mg -AgBr interactions it is clear from the values that χ^2 per degree of freedom value is better at $H < 1$ than $H = 1$. But the values do not fit so well as we confidently say that the fluctuation is self-affine. So next we divide the full bin range into different sub-ranges and calculate χ^2 per degree of freedom for each bin. Values of χ^2 per degree of freedom are given in Table 1. The values of intermittency exponents, which is obtained from the linear fits of the plots, in different bins for that value of

Figures 3(a,b) for $H = 1.0$ and $H = 0.3$ respectively.

Figures are given for that value of H where self-affine or self-similar behaviour is best revealed for that particular range of M .

From the analysis, it is observed that the fluctuation pattern of target fragments is different in different bins. It is highly interesting that the fragmentation process is self-affine ($H = 0.3$) in the bin $15 \leq M \leq 30$, whereas it is

Table 2 The values of $\chi^2/d.o.f$ in different bins for different Hurst exponent H for $^{132}\text{S}-\text{AgBr}$ interactions

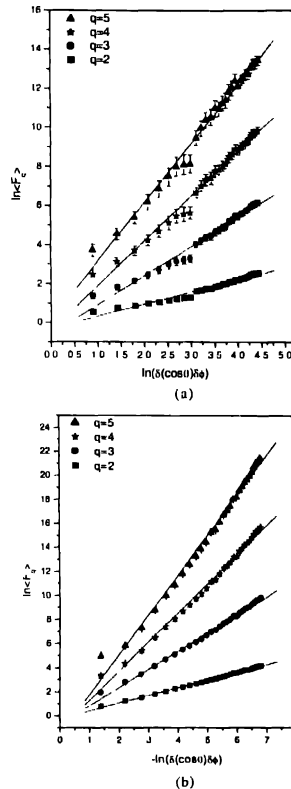
| q | | Values of $\chi^2/d.o.f$ | | | |
|-----|---|--------------------------|--------------------|---------------------|---------------------|
| | | $6 \leq M \leq 26$ | $6 \leq M \leq 16$ | $16 \leq M \leq 26$ | $10 \leq M \leq 20$ |
| 3 | 2 | 0.469 | 0.224 | 0.021 | 0.039 |
| | 3 | 1.163 | 1.109 | 0.016 | 0.119 |
| | 4 | 1.342 | 1.763 | 0.035 | 0.327 |
| 4 | 2 | 0.168 | 0.110 | 0.047 | 0.073 |
| | 3 | 0.635 | 0.343 | 0.051 | 0.284 |
| | 4 | 1.436 | 0.836 | 0.125 | 0.568 |
| 5 | 2 | 0.241 | 0.183 | 0.113 | 0.295 |
| | 3 | 0.849 | 0.256 | 0.323 | 0.539 |
| | 4 | 1.810 | 0.515 | 0.914 | 1.412 |
| 6 | 2 | 0.258 | 0.188 | 0.333 | 0.181 |
| | 3 | 0.889 | 0.829 | 1.091 | 0.292 |
| | 4 | 2.335 | 1.867 | 3.011 | 1.227 |
| 7 | 2 | 0.489 | 0.489 | 0.150 | 0.789 |
| | 3 | 0.972 | 1.034 | 0.850 | 1.265 |
| | 4 | 2.872 | 3.157 | 2.723 | 3.361 |
| 8 | 2 | 0.272 | 0.223 | 0.258 | 0.366 |
| | 3 | 0.649 | 0.579 | 0.541 | 0.465 |
| | 4 | 1.709 | 2.037 | 0.999 | 0.651 |

self-similar in the bins $2 \leq M \leq 15$, $10 \leq M \leq 20$ and $12 \leq M \leq 25$. The values of α_q are different for bins $2 \leq M \leq 30$, $2 \leq M \leq 15$ and $15 \leq M \leq 30$. However, it is identical for bins $10 \leq M \leq 20$ and $12 \leq M \leq 25$.

Thus, we can conclude that the fluctuation pattern of target fragments for $^{24}\text{Mg}-\text{AgBr}$ interactions at 4.5 AGeV is scale-dependent though the strength of the fluctuation does not vary widely in the different bin regions.

Similar analysis was performed in case of $^{132}\text{S}-\text{AgBr}$ interactions.

We have plotted $-\ln(\delta(\cos\theta)\delta\phi)$ along horizontal axis and $\ln\langle F_q \rangle$ along vertical axis for $q = 2-4$ for different Hurst components starting from $H = 0.3$ to $H = 0.7$ by steps of 0.1 and for $H = 1.0$ in bin region

**Figure 1.** Plot of $\ln\langle F_q \rangle$ vs $-\ln(\delta(\cos\theta)\delta\phi)$ for $q = 2-5$ for $^{24}\text{Mg}-\text{AgBr}$ interactions for (a) $H = 1.0$ and (b) $H = 0.3$ in bin range $2 \leq M \leq 30$.

$6 \leq M \leq 26$, $6 \leq M \leq 16$, $16 \leq M \leq 26$, $10 \leq M \leq 20$. Linear best fit was performed and $\chi^2/d.o.f$ was calculated. The slope of the straight line gives the value of intermittency exponent α_q . The values of $\chi^2/d.o.f$ are specified in Table 2. Figures 4(a,b), 5, 6 give the plot of

Table 3 The values of α_q in different bin regions for that particular value of H at which self-similarity or self-affinity occurs for $^{24}\text{Mg}-\text{AgBr}$ interactions

| q | Values of α_q | | | | |
|-----|---------------------------------|---------------------------------|----------------------------------|----------------------------------|----------------------------------|
| | $2 \leq M \leq 30$ $H = 1.0$ | $2 \leq M \leq 15$ $H = 1.0$ | $15 \leq M \leq 30$ $H = 0.3$ | $10 \leq M \leq 20$ $H = 1.0$ | $12 \leq M \leq 25$ $H = 1.0$ |
| 2 | 0.63 ± 0.01 | 0.60 ± 0.01 | 0.80 ± 0.02 | 0.68 ± 0.01 | 0.68 ± 0.01 |
| 3 | 1.51 ± 0.02 | 1.38 ± 0.02 | 1.72 ± 0.04 | 1.64 ± 0.04 | 1.66 ± 0.03 |
| 4 | 2.42 ± 0.04 | 2.19 ± 0.06 | 2.40 ± 0.07 | 2.64 ± 0.06 | 2.70 ± 0.05 |
| 5 | 3.31 ± 0.06 | 2.96 ± 0.10 | 2.82 ± 0.11 | 3.66 ± 0.08 | 3.76 ± 0.06 |

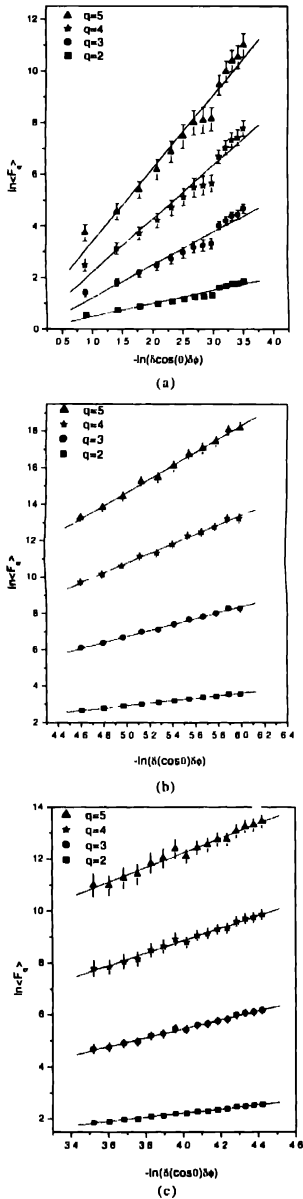


Figure 2. Plot of $\ln\langle F_q \rangle$ vs $-\ln(\delta(\cos\theta)\delta\theta)$ for $q = 2-5$ for $^{24}\text{Mg} - \text{AgBr}$ interactions for $H = 1.0$ in bin range (a) $2 \leq M \leq 30$, (b) $10 \leq M \leq 20$ and (c) $12 \leq M \leq 25$

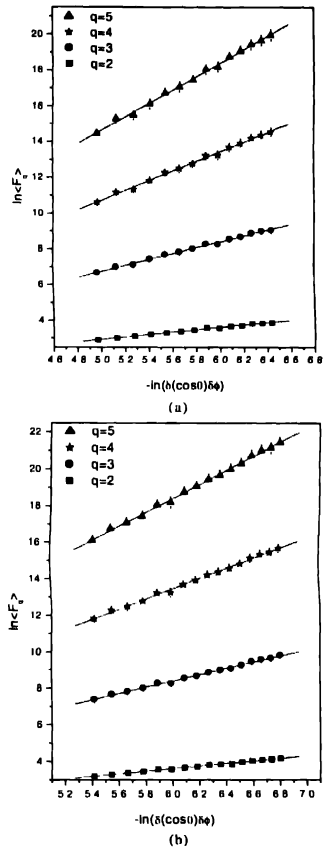


Figure 3. Plot of $\ln\langle F_q \rangle$ vs $-\ln(h(\cos\theta)\delta\theta)$ for $q = 2-5$ for $^{24}\text{Mg} - \text{AgBr}$ interactions for (a) $H = 1.0$ and (b) $H = 0.3$ in bin range $15 \leq M \leq 30$

$\ln\langle F_q \rangle$ vs $-\ln(\delta(\cos\theta)\delta\theta)$ for those values of H for which self-affinity or self-similarity ($H = 1.0$) is observed in the bins $6 \leq M \leq 26$, $6 \leq M \leq 16$, $16 \leq M \leq 26$, $10 \leq M \leq 20$, respectively

We observe that for bins $6 \leq M \leq 26$, the fluctuation pattern is self-affine with Hurst exponent $H = 0.4$, for bins $6 \leq M \leq 16$, fluctuation pattern is self-affine with Hurst exponent $H = 0.5$, whereas for bins $16 \leq M \leq 26$ and $10 \leq M \leq 20$, fluctuation pattern is self-affine with Hurst exponent $H = 0.3$. For $^{24}\text{Mg} - \text{AgBr}$ interactions, the fluctuation pattern is self-similar in most of the bins while self-affine in only one bin region whereas for $^{32}\text{S} - \text{AgBr}$

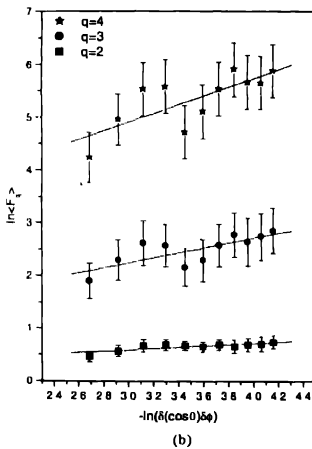
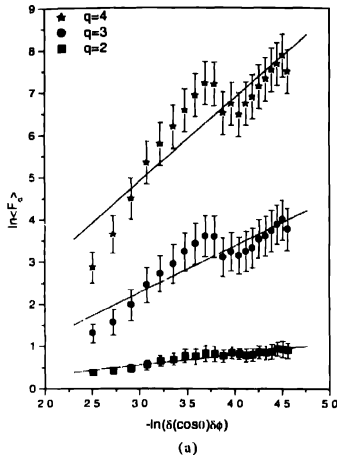


Figure 4. Plot of $\ln\langle F_q \rangle$ vs $-\ln(\delta(\cos\theta)\delta\theta)$ for ^{32}S -AgBr interactions for (a) $H = 0.4$ in bin range $6 \leq M \leq 26$, (b) $H = 0.5$ in bin range $6 \leq M \leq 16$

interactions, the fluctuation pattern is self-affine in all the considered bin regions.

The values of α_q in different bins for that value of H where self-affinity occurs, are given in Table 4. Unlike the case of ^{24}Mg -AgBr interactions at 4.5 AGeV, the intermittency exponent α_q varies widely in the different bin regions. We also find that the values of α_q are higher in the case of ^{32}S -AgBr interactions. Thus, the fluctuation pattern of target fragments for ^{32}S -AgBr interactions at 200 AGeV is scale-dependent too and the dependence is

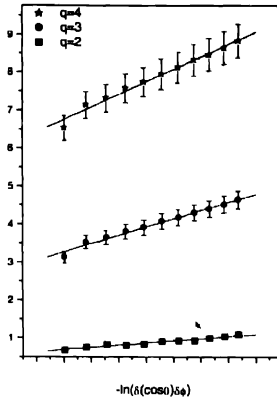


Figure 5. Plot of $\ln\langle F_q \rangle$ vs $-\ln(\delta(\cos\theta)\delta\theta)$ for ^{32}S -AgBr interactions for $H = 0.3$ in bin range $16 \leq M \leq 26$

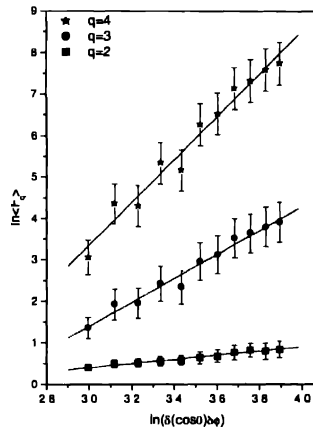


Figure 6. Plot of $\ln\langle F_q \rangle$ vs $-\ln(\delta(\cos\theta)\delta\theta)$ for ^{32}S -AgBr interactions for $H = 0.3$ in bin range $10 \leq M \leq 20$.

Table 4. The values of α_q in different bin regions for that particular value of H at which self-similarity or self-affinity occurs for ^{32}S -AgBr interactions

| | Values of α_q | | | |
|---|---------------------------------|---------------------------------|----------------------------------|----------------------------------|
| | $6 \leq M \leq 26$ $H = 0.4$ | $6 \leq M \leq 16$ $H = 0.5$ | $16 \leq M \leq 26$ $H = 0.3$ | $10 \leq M \leq 20$ $H = 0.3$ |
| 2 | 0.250 ± 0.019 | 0.127 ± 0.030 | 0.575 ± 0.043 | 0.496 ± 0.029 |
| 3 | 1.099 ± 0.112 | 0.471 ± 0.129 | 2.189 ± 0.089 | 2.893 ± 0.149 |
| 4 | 1.971 ± 0.204 | 0.826 ± 0.236 | 3.309 ± 0.143 | 5.163 ± 0.296 |

more pronounced in this case compared to ^{24}Mg -AgBr interactions at 4.5 AGeV.

The conclusion is highly interesting. One observes that for $^{24}\text{Mg-AgBr}$ interaction at 4.5 AGeV in the bin range $2 \leq M \leq 30$ fluctuation pattern appears to be neither self-similar nor self-affine whereas in smaller bins, it is either self similar or self affine. The scenario is altogether different at ultra-relativistic energies. In case of ^{12}S -initiated interaction at 200 AGeV in all bins, self-affinity is evident and degree of anisotropy appears to be different.

Thus, this analysis reveals a very interesting feature of particle production in nuclear collisions.

- (i) The fluctuation pattern for target fragments is *scale* (bin)-dependent both at relativistic and ultrarelativistic energies
- (ii) With increase in the projectile energy, the fluctuation pattern tends to become self-affine rather than self-similar
- (iii) The strength of the fluctuation and also the *scale* (bin)-dependence is more pronounced at ultra-relativistic energy

The possible physical picture one can draw from this paper, is that the evaporation model fails to explain the angular distribution of the target fragments. Another important finding as revealed by the experiment is the target emission process appears to be beam energy-dependent. At lower energy, target emission seems to be self-similar in almost all scales (isotropic phase space) whereas at considerable higher energy emission process becomes totally self-affine (anisotropic phase space). Further, higher energy causes more target excitation revealing more anisotropic phase-space.

Acknowledgements

We thank Prof. K. D. Tolstov of JINR, Dubna, and Prof. P. L. Jain, State University of New York at Buffalo, USA, for giving us the exposed emulsion plates. Two of our authors, Srimonti Dutta and Madhumita Banerjee Lahiri gratefully acknowledge CSIR (India) for financial support.

References

- [1] A. Bialas and R. Peschanski *Nucl. Phys.* **B273** 703 (1986)
- [2] B. I. Hao *Chaos* (Singapore: World Scientific) (1984)
- [3] D. Ghosh *et al*, *Phys. Rev.* **C47** 1120 (1993), P. L. Jain and G. Singh *Nucl. Phys.* **A596** 700 (1996)
- [4] D. Ghosh *et al*, *Phys. Rev.* **C58** 3553 (1998)
- [5] D. Ghosh *et al*, *Phys. Rev.* **C49** R1747 (1994)
- [6] A. Capella, K. Fialkowski and A. Krzywicki *Phys. Lett.* **B230** 149 (1989)
- [7] P. Carruthers and I. Sarcevic *Phys. Rev. Lett.* **63** 1562 (1989)
- [8] W. Ochs and J. Wosiek *Phys. Lett.* **B232** 271 (1989)
- [9] J. Dias de Deus and J. C. Seixas *Phys. Lett.* **B229** 402 (1989)
- [10] C. F. Powell, P. H. Fowler and D. H. Perkins *The Study of Elementary Particles by Photographic Method* (New York: Pergamon) (1963)
- [11] W. H. Barkas *Nuclear Research Emulsion-II* (New York: Academic) (1963)
- [12] W. Ochs *Phys. Lett.* **B247** 101 (1990)
- [13] L. Van Hove *Phys. Lett.* **B28** 429 (1969), *Nucl. Phys.* **B9** 331 (1969)
- [14] D. Ghosh *et al*, *J. Phys.* **G29** 983 (2003)
- [15] D. Ghosh *et al*, *Lett. Phys. J.* **A14** 77 (2002)
- [16] D. Ghosh *et al*, *J. Phys.* **G30** 499 (2004)
- [17] Liu Lianshou, Yan Zhang and Wu Yuanfang *Z. Phys.* **C69** 327 (1996)
- [18] Liu Lianshou, Yan Zhang and You Deng *Z. Phys.* **C73** 535 (1997)